FULLY AUTOMATIC BREAST SEGMENTATION IN 3D BREAST MRI

Lei Wang[⋆] *Bram Platel*[⋆] *Tatyana Ivanovskaya*[†] *Markus Harz*[⋆] *Horst K. Hahn*[⋆]

[⋆] Fraunhofer MEVIS - Institute for Medical Image Computing, Bremen, Germany
[†] Institute for Community Medicine, Ernst-Moritz-Arndt University, Greifswald, Germany

ABSTRACT

In computer-aided diagnosis of breast MRI, a precise segmentation of the breast is often required as a fundamental step to facilitate further diagnostic tasks, e.g., breast density measurement, lesion detection and automatic reporting. In this work, a fully automatic method dedicated to breast segmentation is proposed, which comprises four major steps: sheet-like structures enhancement, pectoralis muscle boundary segmentation, breast-air boundary segmentation and breast extraction. To validate the proposed method, the segmented breast boundaries of 84 breast MR images, acquired in five different sites with variant imaging protocols, were compared to the manual segmentation. An average distance of 2.56mm with a standard deviation of 3.26mm was achieved.

Index Terms— breast MRI, breast segmentation, Hessian filter, region growing

1. INTRODUCTION

Breast MR is an invaluable tool in the clinical work-up of patients suspected of having breast cancer [1]. Moreover, breast MRI is gaining popularity as a screening modality for high-risk patients with BRCA 1 & 2 gene mutations or dense breasts [2]. A multitude of computer-aided diagnostic methods and tools have been developed aiming to assist the radiologists and physicians in automatic reporting, density analysis, and breast lesion detection. Normally, a precise segmentation of the breast is required and serves as a fundamental step to avoid processing irrelevant structures, such as background and the thoracic organs, which confines the CAD systems to focus on the breast tissue and thus improve the efficiency and accuracy by eliminating false positives outside the breast tissue.

Normally, the task of breast segmentation is divided in two steps: the identification of breast-air boundary and pectoralis muscle boundary. Koenig et al. presented a thresholding based algorithm to detect breast-air boundary [3], which might have difficulties when the aliasing artifacts or fiducial markers are presented. Giannini et al. recently introduced a method which highly relies on the prior anatomical knowledge of pectoralis muscle [4]. Nie et al. used fuzzy C-mean classification to segment breast, where the aortic arch was initialized by users as a landmark. The method might fail, particularly in coronal acquisitions where the aortic arch is not imaged [5].

In this work, we propose a novel solution for breast segmentation in MR acquisitions, which does not require any anatomical landmarks. It is specially designed for processing non-fat suppressed breast MRI, where fatty tissue has a high intensity level compared to parenchyma and pectoralis muscle. The method is based on the key observation that the pectoralis muscle and breast-air boundaries exhibit smooth sheet-like surfaces in 3D, which can be simultaneously enhanced by a Hessian-based sheetness filter [6]. The enhancement strength of the designed Hessian-based filter correlates with the shape and contrast information of the structures, which means that structures with non-specific shapes and lower contrast will be suppressed. The overall framework consists of four major steps: enhancement of the sheet-like structures, segmentation of the pectoralis muscle boundary defining the lower border of the breast region, segmentation of the breast-air boundary delimiting the upper border of the breast region, and breast extraction which eventually captures the area of breast tissue.

2. METHODS

The schematic overview of the entire segmentation work-flow is depicted in Fig. 1, and the details of each major step are described in the following sections.

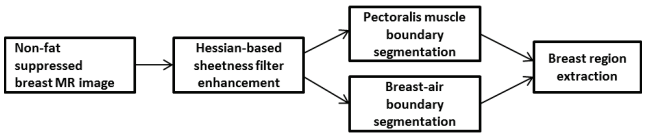


Fig. 1. Work-flow of the method.

2.1. Sheet-like structures enhancement

Hessian-based filters are typically used to enhance and differentiate structures with specific shapes, i.e., blobs, sheets and tubes. By properly manipulating the relations of the eigenvalues, a filter defined to enhance the structures with a specific shape can assign each voxel with a likelihood value scaled from 0 and 1, representing how likely the voxel belongs to the corresponding shape, given its spatial neighborhood. In [7], a Hessian-based sheetness filter was developed to segment

the pectoralis muscle boundary. In this work, the prominent sheet-like structures are enhanced with the same sheetness measurement filter, which is defined in the following equation assuming the Eigenvalues are sorted in $|\lambda_1| \geq |\lambda_2| \geq |\lambda_3|$:

$$S = \begin{cases} 0, & \text{if} \quad \lambda_1 = 0, \\ \exp\left(\frac{-R_{sheet}^2}{2\alpha^2}\right)\left(1 - \exp\left(\frac{-R_{noise}^2}{2\beta^2}\right)\right) & \text{otherwise}, \end{cases}$$

where $R_{sheet} = |\lambda_2|/|\lambda_1|$, and $R_{noise} = \sqrt{\lambda_1^2 + \lambda_2^2 + \lambda_3^2}$. The parameters α and β control the sensitivity of each ratio to the measure, which are set to 0.5 and half of the maximum R_{noise} respectively. The sheetness measure S gives a high response to the sheet-like local structures and suppresses all other structures with low scores. As a second derivative filter, the defined Hessian-based filter results in a zero-crossing on the target boundaries (step edges) and maximal response on both upper and lower sides of the edges. By differentiating the sign of the largest Eigenvalue, only the voxels enhanced on the dark region are kept.

2.2. Pectoralis muscle boundary segmentation

The identification of the pectoralis muscle boundary is necessary when separating the irrelevant thoracic organs from the breast tissue. The fully automatic method implemented in [7] is adopted in this work. The method first generates a region of interest (ROI) which covers the pectoralis muscle by selecting a specific range of gradient directions of the enhanced sheet-like structures. Then, a vector-based connected component filter, which takes the Eigenvectors into considerations, is employed to further segment the pectoralis muscle boundary more accurately. In addition, the method is capable of handling cases where the parenchyma is quite close to the pectoralis muscle in dense breasts. We tested the algorithm with datasets collected from multiple sites, and the quantitative validation is depicted in Section 3.

2.3. Breast-air boundary segmentation

Breast-air boundary segmentation is not a trivial task due to artifacts that can appear in MR images, such as the presence of aliasing artifacts and fiducial markers, which might cause failure of intensity based methods. In addition, the absence of one breast due to mastectomy surgery might also challenge the model based methods (see Fig. 2).

Compared to the response of the pectoralis muscle boundary, the breast-air boundary is enhanced even stronger by the sheetness filter, which obtains a sheetness score mostly higher than 0.9, due to the high contrast between air and breast tissue. The mask of the pectoralis muscle segmented in the previous step can remove the thoracic region of the Hessian filter response, which facilitates the segmentation of the breast-air boundary (Fig. 3(a)(b)). By thresholding the remaining enhanced structures with a minimum threshold of 0.8 on S, unwanted objects slightly enhanced inside the breast can be

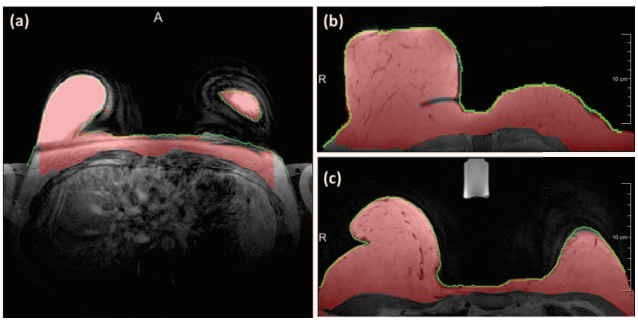


Fig. 2. The artifacts and challenges presented in breast MRI, overlaid with the segmented breasts (red masks), and the reference breast-air boundaries annotated by a radiologist (green contours): (a) Presence of aliasing artifacts (ghost shadow). (b) Absence of the left breast. (c) Presence of fiducial markers

filtered out. Then, a 3D vector-based connected component algorithm is applied to extract the largest connected component, which is the breast-air boundary (Fig. 3 (c)). The algorithm takes the Eigendirections, of the voxels into consideration and inspects the connectedness with not only spatial connectivity but also the consistency of the Eigendirections. This enables the algorithm to isolate the attached parenchyma from the breast boundary. Another observation is that the segmented breast-air boundary normally has a thickness larger than one single voxel resulting from the scale of the Hessian filter. However, by properly setting the scale, the segmented boundary can be acquired sufficiently close to the true boundary. In this work, the input image is down-sampled with an isotropic voxel size of 2.5mm, and the scale parameter of the Hessian filter is set to 2.5mm (1 voxel) as well. The accuracy of the segmented breast-air boundaries is tested and shown in Section 3.

2.4. Breast segmentation

The segmented breast-air and pectoralis muscle boundaries delimit the upper and lower borders of the breast tissue, which already allows for capturing an initial segmentation of the breast tissue. (Fig. 3(d)). However, in extreme inferior slices where the visible breast tissue is not directing connected to the body (see Fig. 2(a)), the connected component algorithm may lose the breast tissue. In addition, the local misalignment of the detected pectoralis and breast-air boundaries may cause the breast tissue extraction to deviate locally from the true borders. To cope with this issue and refine the breast tissue segmentation in local areas, an intensity based region growing algorithm is adopted, working on the basis of the initial breast segmentation.

Firstly, the seeds of the region growing are automatically identified by analyzing the distance transform image of the initial breast segmentation (Fig. 3(e)). The voxels with high distance transform values are distributed around the geomet-

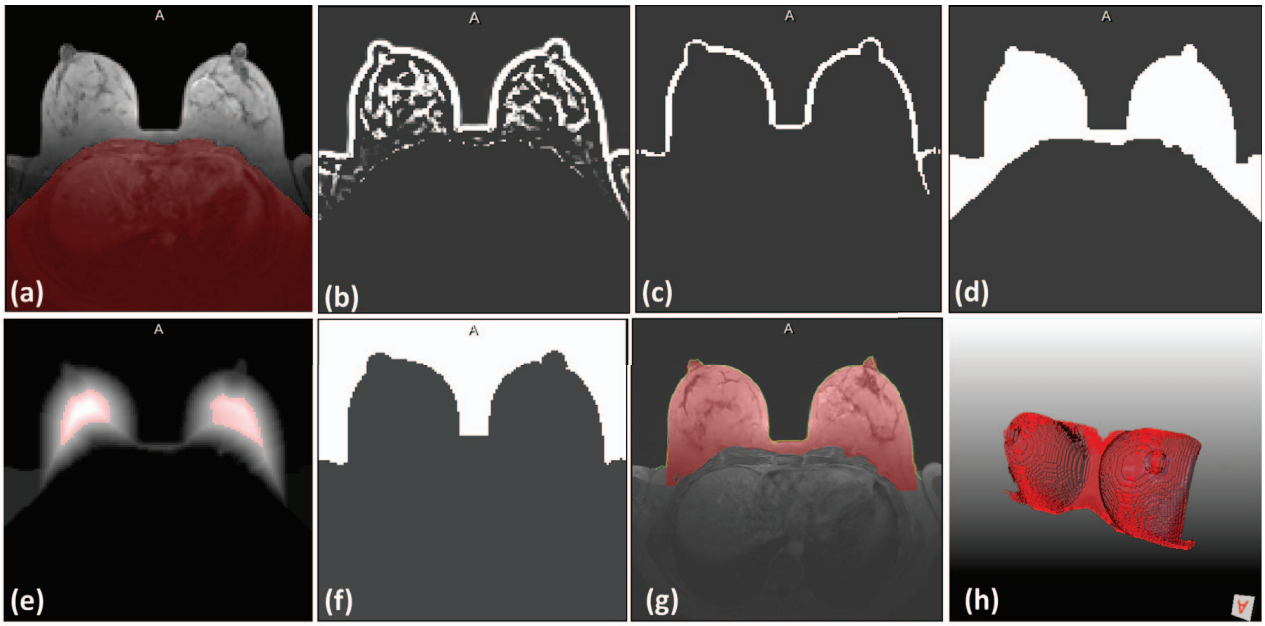


Fig. 3. The breast-air segmentation and the breast extraction: (a) Original input overlaid with pectoralis muscle segmentation (red mask); (b) Masked Hessian filter response where breast-air boundary is highly enhanced; (c) Breast-air boundary segmented with connected component and morphological filters; (d) Initial breast tissue segmentation using segmented breast-air and pectoralis muscle boundaries; (e) Seed voxels (encoded in red) extracted from distance transform image of the initial segmentation; (f) Air background detection based on the initial segmentation; (g) (h) 2D and 3D demonstration of segmented breast tissue

ric center of the initial segmentation. More specifically, we choose the voxels above the 70 percent quantile of the histogram of distance transform values as the seeds (encoded in red overlay in Fig. 3(e)) . Secondly, three constraints are implemented to ensure that the region growing propagates within the breast and prevent leakages into the thorax and air. The detected pectoral muscle and breast-air boundaries are superimposed to the original input and the intensities of the covered voxels are set to zero, aiming to block the growing process. In addition, the intensity level of the air background is investigated by first segmenting the air region using a ray tracing technique, where the rays are emitted from the top of the image and travel downwards until hitting the segmented breast-air boundary (Fig. 3(f)), and then analyzing the intensity histogram. The lower threshold of the region growing is safely set as the mean of this histogram plus three times the standard deviation. The region growing process makes the assumption that the breast parenchyma possesses higher intensities than air background. However, in a few rare cases, where the patient suffered from surgical biopsy or tumor resection, the operated sites might exhibit similar low signals as the background, which results in a few small-scaled holes or cavities inside the breast uncovered by region growing. Since these cavities are surrounded by fatty tissue, they can be easily recovered by hole-filling techniques, such as morphological closing and connection cost filters. Ultimately, the segmentation result of the region growing is demonstrated in 2D (Fig. 3(g)) and visualized in 3D (Fig. 3(h)).

3. RESULTS AND EVALUATIONS

To evaluate the performance of the presented method, a test data set enclosing 84 non-fat suppressed breast MR images was collected. The test images were acquired in five different hospitals with different imaging protocols, i.e., T1-coronal, axial, sagittal, T2-axial. Only the pre-contrast images were processed for dynamic contrast enhanced images. The image resolution varied from $256 \times 256 \times 64$ to $512 \times 512 \times 80$ with different voxel sizes. The reference segmentations were manually annotated by an experienced radiologist. For each test image, two individual reference contours, delineating the pectoralis muscle boundary and the breast-air boundary, were annotated, and the combined contours were used as the reference boundaries of the breast. Considering the resolution and slice numbers of the data, the radiologist annotated the breast-air and pectoralis muscle boundaries for every second to eighth slice to make sure that at least 15 equally distributed annotated slices were provided. The processing time for the image with maximum resolution was about 20 seconds using a 3.07 GHz Intel CPU and a GeForce gtx285 graphics card.

The boundary contours of the breast-air and the pectoralis

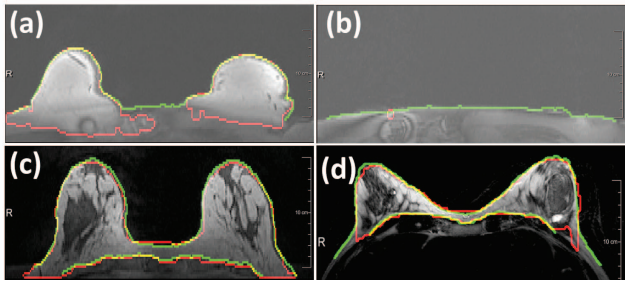


Fig. 4. The segmented pectoralis and breast-air boundaries (red), the reference contours (green), the overlap contours (yellow)

muscle were extracted from the segmented region of the breast. We measured the distances from the reference contours to the segmented contours in the slices where reference contours exist. The distance from each voxel in the reference contour to the segmented contour was measured, and the mean, standard deviation, and maximum of the distance error of each test image were computed. In addition, an average overlap rate, defined as the percentage of the reference voxels whose distance error was less than a tolerance threshold of 3mm, was evaluated.

Two experiments were carried out to validate the segmentation accuracy of the pectoralis muscle and the breast-air boundaries by comparing to the corresponding reference boundaries, respectively. Moreover, the accuracy of the segmented breast boundaries was assessed by comparing to the reference boundaries of the breast in the third experiment. Table 1 lists the average values of the evaluation metrics obtained in each experiment for all test images. From the test, it is observed that the pectoralis muscle boundary possessed higher accuracy than the breast-air boundary, with a lower mean distance error and standard deviation. For the entire breast boundary, the method achieved a mean distance of 2.56mm with a standard deviation of 3.26mm. The overlap rate reached 87% on average. The relatively larger average maximum distance recorded as 33.56mm resulted from the deviations in the extremely inferior slices, where for instance the segmented breast-air boundaries were isolated while the radiologist annotated a continuous reference breast-air boundary crossing the muscles (Fig. 4(a)), no breast tissue volume was presented while the radiologist annotated a continuous reference pectoralis muscle boundary (Fig. 4(b)). To demonstrate the results, two segmented breast boundaries for dense breasts are illustrated in Fig. 4(c)(d), and the segmented breast masks of the forenamed challenge cases are showed in Fig. 2.

4. CONCLUSIONS AND DISCUSSIONS

In this paper, a fully automatic method of breast tissue extraction in non-fat suppressed breast MR images is presented.

Boundary	Mean(mm)	Std(mm)	Max(mm)	O.R.
Pectoralis	1.99	2.66	22.16	0.92
Breast-air	2.81	3.22	30.47	0.84
Breast:	**2.56**	**3.26**	**33.56**	**0.87**

Table 1. The average values of the evaluation metrics validating the segmentation accuracy of the pectoralis muscle boundary, breast-air boundary and both (the breast boundary), where O.R indicates overlap rate

An extensive test including 84 data sets was carried out to assess the performance of the algorithm. By analyzing the test results, the designed Hessian-based sheetness filter was proven to be an accurate and robust tool for enhancing major sheet-like structures: the breast-air and the pectoralis muscle boundaries. The automatic initialization of the seed points and the analysis of the lower threshold of the proposed region growing technique have proven their robustness on the clinical data. The boundaries of the extracted breast region showed a high alignment with the reference contours annotated manually with an overlap rate of 87%. In the future, significant parameters of the presented pipeline, such as the thresholds of the sheetness filter response, will be further optimized.

5. REFERENCES

[1] J. G.M. Klijn, "Early diagnosis of hereditary breast cancer by magnetic resonance imaging: What is realistic?," *Journal of Clinical Oncology*, vol. 28, no. 9, pp. 1441–1445, 2010.

[2] A. J. Rijnsburger et al., "Brca1-associated breast cancers present differently from brca2-associated and familial cases: Long-term follow-up of the dutch mrisc screening study," *Journal of Clinical Oncology*, vol. 28, no. 36, pp. 5265–5273, 2010.

[3] M. Koenig et al., "Automatic segmentation of relevant structures in DCE MR mammograms," *Proceedings of SPIE*, 2007.

[4] V. Giannini et al., "A fully automatic algorithm for segmentation of the breasts in DCE-MR images.," *Proceedings of EMBS*, vol. 2010, pp. 3146–9, Jan. 2010.

[5] K. Nie et al., "Development of a quantitative method for analysis of breast density based on three-dimensional breast MRI," *Medical physics*, vol. 35, pp. 5253, 2008.

[6] A. Frangi et al., "Multiscale vessel enhancement filtering 1 Introduction 2 Method," *Proceedings of MICCAI*, vol. 1496, pp. 130–137, 1998.

[7] L. Wang et al., "Fully automated segmentation of the pectoralis muscle boundary in breast MR images," *Proceedings of SPIE*, vol. 7963, pp. 796309–796309–8, 2011.